

bradscholars

Two-dimensional finite element analysis investigation of the heat partition ratio of a friction brake

| | |
|---------------|--|
| Item Type | Article |
| Authors | Qiu, L.;Qi, Hong Sheng;Wood, Alastair S. |
| Citation | Qiu L, Hong-Sheng Q and Wood A (2018) Two-dimensional finite element analysis investigation of the heat partition ratio of a friction brake. Proceedings of the Institution of Mechanical Engineers, Part J: Journal of Engineering Tribology. 232(12): 1489-1501. |
| DOI | https://doi.org/10.1177/1350650118757245 |
| Rights | The final, definitive version of this paper has been published in Proceedings of the Institution of Mechanical Engineers, Part J: Journal of Engineering Tribology by SAGE Publications Ltd, All rights reserved. © 2018 IMechE. |
| Download date | 2025-07-25 04:14:18 |
| Link to Item | http://hdl.handle.net/10454/14280 |

Original Article

Corresponding author info

*Corresponding Author:

Hong-Sheng Qi, University of Bradford, Richmond Road, Bradford, BD7 1DP, UK

Email: h.qi@bradford.ac.uk

2-D FEA investigation of the heat partition ratio of a friction brake

¹ Qiu, Le; ¹ Qi, Hong-Sheng*, ¹ Wood, Alastair

¹University of Bradford, Bradford, United Kingdom,

Abstract

A 2D coupled temperature-displacement FE model is developed for a pad-disc brake system based on a restricted rotational pad boundary condition. The evolution of pressure, heat flux, and temperature along the contact interface during braking applications is analysed with the FE model. Results indicate that different rotational pad boundary conditions significantly impact the interface pressure distribution, which in turn affects interface temperature and heat flux distributions, and suggest that a particular pad rotation condition is most appropriate for accurately modelling friction braking processes. The importance of the thermal contact conductance in the analysis of heat transfer in friction braking is

established, and it is confirmed that the heat partition ratio is not uniformly distributed along the interface under normal and high interface thermal conductance conditions.

Keywords

Finite element analysis, disc braking, heat transfer, heat partition, thermal contact conductance, pad rotational DOF, interface contact pressure and temperature.

Notation

| | | |
|-------|--------------------|--|
| A_j | m^2 | Contact area of body j |
| A_a | m^2 | Apparent contact area |
| A_r | m^2 | Real contact area |
| c | J/kgK | Specific heat capacity |
| f | | Heat generation ratio |
| h | W/m ² K | Convective thermal conductance (convective heat coefficient) |
| h_c | W/m ² K | Thermal contact conductance (contact heat coefficient) |
| j | | Semi-infinite body, $j = 1,2$ |
| k_j | m ² /s | Thermal diffusivity of body j |
| K_j | W/mK | Thermal conductivity of body j |
| p | Pa | Contact pressure |
| q | W/m ² | Heat flux |
| q_1 | W/m ² | Heat flux into the pad |
| q_2 | W/m ² | Heat flux into the disc |
| R_c | K/W | Thermal contact resistance |
| t | s | time |
| T_0 | °C | Sink temperature |

| | | |
|----------|-------------------|---|
| T_P | °C | Predefined temperature |
| T_j | °C | Transient temperature of semi-infinite body j |
| v | m/s | Relative velocity of the sliding bodies |
| x | m | Distance from the interface |
| α | m/mK | Coefficient of thermal expansion |
| μ | | Coefficient of dynamic friction |
| γ | | Heat partition ratio |
| ρ | kg/m ³ | Density |

Abbreviations

| | |
|-----|---------------------------|
| 2D | Two dimensional |
| 3D | Three dimensional |
| DOF | Degree of freedom |
| FE | Finite element |
| FEA | Finite element analysis |
| FR | Free-Rotation (condition) |
| HPR | Heat Partition Ratio |
| ITL | Interface tribo-layer |

| | |
|----|------------------------------|
| LR | Limited-Rotation (condition) |
| NR | No-Rotation (condition) |

1 Introduction

During a braking event most of the mechanical energy of a moving vehicle is converted into heat through friction between the brake disc/pad friction pair, and 99% of this heat energy is dissipated through the pair [1]. The temperature of the brake components rises after braking applications, which in turn can affect braking performance [2,3]; e.g. an increase in the temperature of brake system components may cause a decrease in the friction coefficient [4]. Poor braking performance, such as brake fade, thermal cracking, and thermally-excited vibration can all be a consequence of these elevated temperatures [2,5]. Thus, it is very important to be able to accurately predict the potential temperature rise of a given brake system and assess the impact upon braking performance.

The potential temperature increase of a brake system is influenced by the nature of the brake disc/pad contact during braking. A better understanding of the disc/pad contact nature, and representing it adequately in modelling/simulation of braking heat transfer, will result in a more accurate prediction of the interface temperature of a given brake system. The main objective of this research is to clarify how the imperfect disc/pad contact nature affects heat partitioning in friction braking. FE analysis is a proven and effective method to study the behaviour of friction brakes in terms of stress/strain, temperature, thermos-elastic instability, vibration/noise, and service life in vehicle braking. Different approaches and assumptions have been used for model simplification in different FE analyses [6–12]. In this investigation a 2D FE model is used to simulate and visualise the brake interface

temperature and heat partition ratio during friction braking under different contact conditions.

2 Literature review

2.1 Interface tribo-layer (ITL) and imperfect thermal contact

It is known that the contact between the disc and the pad is imperfect, from mechanical and thermal perspectives, on several counts. For instance, the contact surfaces are rough rather than smooth; the real contact area A_r is smaller than the apparent contact area A_a (i.e. $A_r < A_a$); the operating environment (e.g. dust, water and contamination) affects the interface contact condition. However, the most significant factor to be considered in analysing a braking process is the formation of an interface tribo-layer (ITL) [2,6,9,12]. It is common practice in braking that bedding-in and burnishing is necessary for any new disc/pad friction pair to enlarge and stabilise the actual contact area by the formation of secondary plateaux and an interface tribo-layer (ITL) [2,7,12-17]. The ITL has different material properties to the contact pair as a result of physical and chemical reactions during braking, such as wear and detached particles. The thickness and the distribution of an ITL depend on many factors.

The existence of an ITL affects heat transfer across the braking interface, similar to the effect of the rough surface contact (i.e. $A_r < A_a$) [18]. Accurate predictions of temperature and pressure distributions in a brake system require consideration of these imperfect interface thermal contact conditions since, when heat flows across the imperfect interface, a temperature discontinuity occurs at the interface [19]. Work by Loizou [20] and Majcherczak et al. [21] showed the importance of including the ITL in analytical studies and/or FE modelling/simulations.

2.2 Thermal contact conductance, h_c

To represent the imperfect contact condition in modelling studies of friction braking heat transfer, thermal contact conductance, h_c (or thermal contact resistance, R_c) has been used [12, 22, 23]. Thermal contact conductance is not a material property and is not a constant. h_c can vary depending on application conditions and is affected by many factors, such as contact pressure/load, sliding speed, contact temperatures, the material properties of the friction pair, and the existence of an ITL [24,25]. For example, an experimental investigation to quantify the interface thermal contact conductance [24] showed that the thermal contact conductance was influenced by the operational history, where loaded/unloaded cycles for pressures 0.845-6.425 MPa were applied. The thermal contact conductance was increased by up to 16% during the first five load cycles and a further 2% by the 30th cycle. It is therefore difficult to quantify the thermal contact conductance, h_c .

Values of h_c from 10^3 to 10^5 W/m²K are reported in literature [5,7,23-26], which agree well with the conductance values for common engineering applications. For example, in an experimental study examining thermal contact resistance and total resistance of metal (SS304)/silicone rubber/SS304 joints under light loads (0.02 to 0.25 MPa of apparent stress) for different heat flux inputs (2.4 to 8.6 kW/m²) [26], values between 0.5×10^3 and 1×10^3 W/m²K were reported as being good estimates for such a low pressure and low heat flux test condition. In comparison, much higher values of contact pressure (~ 0.1 to 10 MPa) and heat flux (~ 0.5 to 50 MW/m²) are expected in conventional friction braking applications. Loizou [20] and Majcherczak [21] defined thermal contact conductance in friction braking based on the thermal conductivity and thickness of the ITL, and/or the composition of the ITL. An ITL with thickness 5-10 μm was observed in some experimental investigations [13,17]. A thermal

contact conductance of 1.974 MW/m²K was recommended by Loizou [20]. In an earlier study, the authors used several values of thermal contact conductance ($h_c = 10^3, 10^4, 10^6$ and 10^9 W/m²K) in an analysis of the sensitivity of h_c value on the braking interface temperature [27].

In order to investigate the thermal contact conductance effect in this work, it is assumed that the thermal contact conductance, h_c , is 10^4 W/m²K as a normal value for conventional friction braking applications, even though much higher and much lower values are possible/applicable in real applications.

2.3 Friction induced heat transfer and heat partition ratio, γ

The concept of the heat partition ratio was introduced in 1937 by Blok [28] and is commonly used in the study of friction induced heat transfer problems.

Heat flux, q , is defined as the friction induced heat per unit area of friction surface per unit time (or the friction power per unit area of friction surface),

$$q = \mu v p \quad (1)$$

μ denotes the coefficient of dynamic friction, v is the relative velocity of the sliding bodies, and p is the contact pressure.

At steady state with no heat dissipation into the surrounding environment at the interface,

$$q = q_1 + q_2 \quad (2)$$

q_1 is the heat dissipated into the pad, q_2 is the heat dissipated into the disc, and γ is the heat partition ratio.

$$q_1 = \gamma q \text{ and } q_2 = (1 - \gamma)q \quad (3)$$

Under transient conditions the temperature, T_j , for the semi-infinite body, j , with heat flux q_j applied at the contact surface can be determined by equation (4), from Carslaw and Jaeger [29],

$$T_j(x, t) = \frac{2q_j\sqrt{k_j t}}{K_j} \cdot \operatorname{ierfc}\left(\frac{x}{2\sqrt{k_j t}}\right) \quad (4)$$

x , t , k_j , and K_j are, respectively, distance from the contact surface, time, thermal diffusivity, and thermal conductivity of the material of the semi-infinite body, j . This equation is used for two bodies ($j = 1, 2$) in contact at $x = 0$ with the frictional heat flux $q = q_1 + q_2$ generated at the interface. Equation (4) is based on the assumption that the two semi-infinite bodies in contact have equal temperature at the interface, i.e. thermal contact conductance $h_c = \infty$ or thermal contact resistance $R_c = 0$. Consequently, the heat partition ratio, γ , is given by equation (5), the so-called Charron's formula,

$$\gamma = \frac{\sqrt{K_1 \rho_1 c_1}}{\sqrt{K_1 \rho_1 c_1} + \sqrt{K_2 \rho_2 c_2}} \quad (5)$$

For a disc brake friction pair where the pad contact area A_1 , is much smaller than the disc swept area, A_2 , the heat partition ratio in braking system is given by equation (6),

$$\gamma = \frac{\left(\frac{A_1}{A_2}\right)\sqrt{K_1 \rho_1 c_1}}{\left(\frac{A_1}{A_2}\right)\sqrt{K_1 \rho_1 c_1} + \sqrt{K_2 \rho_2 c_2}} \quad (6)$$

$\left(\frac{A_1}{A_2}\right)$ is the contact area ratio. Equations (5) and (6) indicate that the heat partition ratio is a constant if the material thermal properties for the friction pair (density ρ , specific heat capacity c , and thermal conductivity K) are constant. However, some research shows that the partition ratio is not a constant but varies along the contact interface, particularly in friction braking applications [12, 30]. It is anticipated that the magnitude and distribution of the heat partition ratio, γ , is affected by many factors in braking, such as the relative velocity

of the moving body, the interface contact length, ITL, the thermo-physical properties of the two bodies in relative sliding, the Peclet number, and the mechanical boundary conditions of the contacting bodies'. The nature of these influences are clarified by means of 2D finite element modelling/simulation through this work.

2.4 Heat generation ratio, f and heat partition models

Day and Newcomb [6] examined the role of interface contact resistance in the calculation of heat flow and temperature generated in brake friction pairs using a 'five-phase model': Phase 1: virgin friction material; Phase 2: reaction zone; Phase 3: surface char layer; Phase 4: Interface layer; Phase 5: metal mating body. They postulated that frictional heat is generated in the friction material (the softer of the friction pair) and transferred across the interface to the rotor. The interface layer (Phase 4) plays an important role in predicting interface temperatures and heat flows. Similar work on how the friction heat is generated and dissipated at and adjacent to the contact interface has been carried out [12, 27, 31-33]. Schaaf [31] assumed that heat generation depended upon the type of friction interface, i.e. lubricated/wet friction or dry friction. Under a lubricated condition the friction heat is generated at the middle of the lubrication film. Under a dry condition the friction heat is generated on each of the two contact surfaces, i.e. there are two heat fractions, $f q$ and $(1 - f)q$, separated by a single friction layer, where f is the heat generation ratio and q is the friction induced heat flux. Nosko et al. [32] assumed that generated friction heat had two basic components, adhesive (interfacial bonds between the bodies) and deformational (deformation of roughness asperities and neighbouring volumes of materials), where the deformational component contributed to volume heat generation in the subsurface layers. As Barber pointed out [33], the heat generated during sliding is associated with plastic deformation caused by mechanical interaction between the solids at or near the actual

contact areas, and the plastic deformation that results in heat generation extends some depth below the contact surface. The exact location of the heat source become important if the metallic contact at the interface is reduced by oxide layers [33]. In other words, if there is a zero thermal resistance (metallic contact) at the contact interface (ignoring effects of ITL, oxide layers, and imperfect contact), then the location of friction heat generation becomes insignificant as far as heat transfer/partition is concerned. Although the value of f within a braking process is still not clear, it is reasonable to argue that the value of f should lie between 0.5 to 1 in a friction braking process. This is based on the fact that more heat is expected to be generated at the pad side since the pad material is softer and therefore more easily to be deformed (plastically) and worn than the steel disc [6, 27, 35]. The authors carried out a preliminary study where values $f = 0.5, 0.75$, and 1 were used to analyse the sensitivity of f on the heat transfer and interface temperature [27]. $f = 0.75$ is assumed in this work (i.e. 75% of the heat flux is generated at the pad side), even though higher or lower values are possible/applicable in real applications.

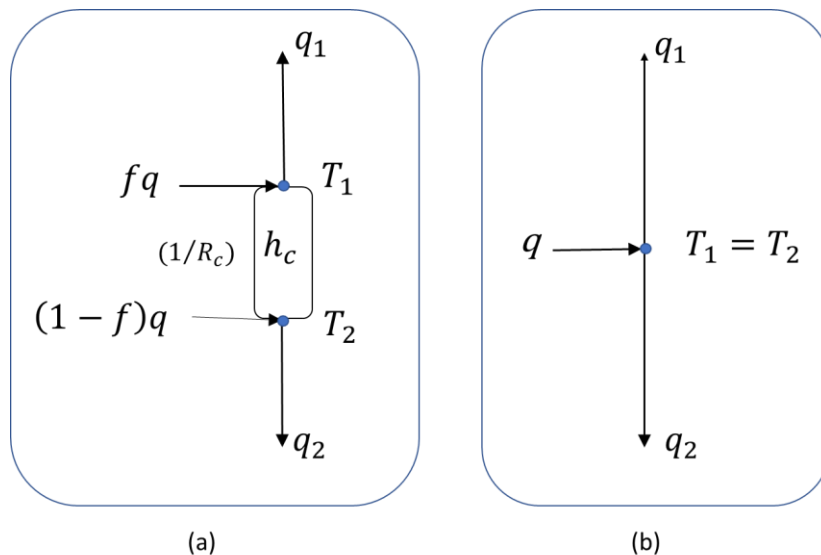


Figure 1. Friction pair heat partition models adapted from [32], (a) for imperfect thermal contact, and (b) for perfect thermal contact.

There are several heat partition models reported [6, 20, 22, 28, 29, 30-34] and two typical models are adapted here from Nosko et al. [32], shown in Figure 1. The model in Figure 1(a) illustrates how factors, particularly the heat generation ratio f and the thermal contact conductance h_c (or its inverse interface thermal resistance, R_c), may affect the heat transfer in a friction braking process. By comparison, Figure 1 (b) provides a representation of the conventional friction-pair heat partition model that is described by equations (2-6). The model shown in Figure 1(a) is used to describe the 2D FE model developed in the present work, particularly the imperfect disc/pad contact interface.

3 Numerical method and FE 2D model setup

3.1 Basic model settings and material properties

ABAQUS software is used for the 2D FE modelling.

The size of the pad in the FE model has dimensions $L \times H = 30 \text{ mm} \times 15 \text{ mm}$ (shown in Figure 2) based on a small-scale test rig used for corresponding experiments (shown in Figure 3) [20]. The disc length in the FE model is 200 mm (equivalent to the disc sliding against the pad for one revolution in 33 ms under the experimental condition) and 1000 mm (set up for the analysis of transient or steady state heat transfer/partitioning during a friction application of 190 ms), respectively. The minimum element size in this FE model is 0.30 mm adjacent to the contact surface. The maximum element size is 1.25 mm adjacent to the disc's lower surface and pad back plate (shown in Figure 2). The CPE4T 4-node plane-strain element is used (thermally coupled quadrilateral, bilinear displacement and temperature).

Table 1. 2D FE Model settings (mechanical and thermal)

| Model settings | |
|---|--------------------------------------|
| Heat generation, f | 0.75 |
| Friction coefficient, μ | 0.4 |
| Load, ρ (MPa) | 1 |
| Sink temperature, T_0 ($^{\circ}$ C) | 20 |
| Predefined temperature, T_p (C) | 100 |
| Degree of Freedom (Pad) | NR, FR (At Pivot A), LR (At Pivot D) |
| Thermal conductance, h_c (W/m ² K) | $10^4, 10^6$ |
| Disc sliding speed, v (m/s) | 5 |
| Time instant (ms) | 33, 190 |
| Contact area ratio $\left(\frac{A_1}{A_2}\right)$ | 3/20 |

Other settings are listed in Table 1, e.g. $f = 0.75$ is used based on the discussion in section

2.4. The material properties are listed in Table 2.

Table 2. Material properties [20]

| | Disc | Pad | Back Plate |
|---|------|------|------------|
| Thermal Conductivity k (W/mK) | 48 | 2.06 | 41.5 |
| Density ρ (kg/m ³) | 7800 | 2580 | 7800 |
| Young's Modulus (GPa) | 209 | 1.25 | 210 |
| Poisson's Ratio | 0.3 | 0.3 | 0.34 |
| Thermal Expansion α (m/mK) x 10^{-6} | 11 | 14.3 | 11 |
| Specific Heat c (J/kgK) | 452 | 749 | 480 |

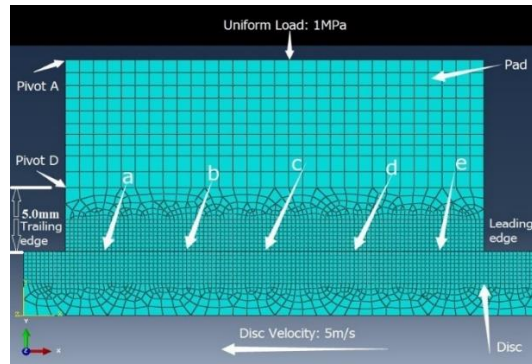


Figure 2. 2D model settings with pivot points A and D along the pad's trailing edge.

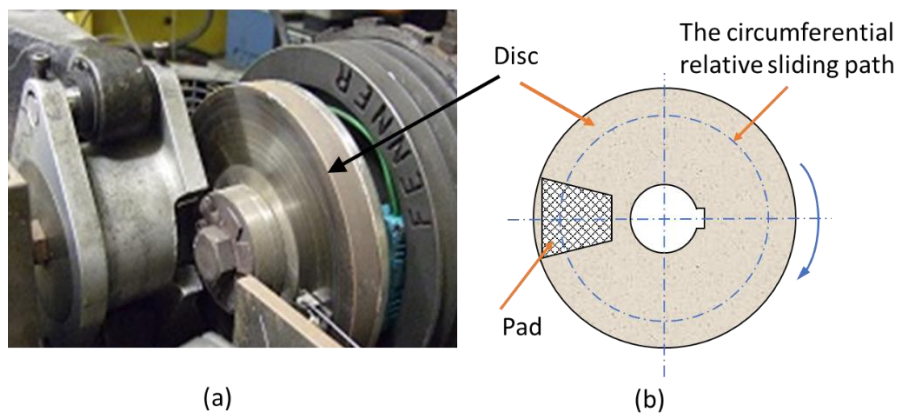


Figure 3. (a) Small-scale test rig used in the investigation [20]. (b) Circumferential relative path of the disc sliding with respect to the pad, represented in the FE model (Figure 2).

3.2 Thermal contact conductance

As discussed in section 2.2, it is assumed that a normal value for the thermal contact conductance, h_c , is 10^4 W/m²K in conventional friction braking applications. At the same time, to represent more idealised interface thermal conditions, a higher value of 10^6 W/m²K is used for comparison purposes.

It is known that the thermal contact conductance is affected by the existence of local gaps at a micro level scale between the pad and disc contact surfaces, such as the disc run out, roll

back and surface roughness of the disc/pad contact surfaces, R_a [6, 15, 20]. In this work the effective clearance between the pad and disc contact surfaces, used in setting up the FE interface condition, lies between 0 and 10 μm , based on the fact that R_a is around 0.5 to 50 μm . Figure 4 shows the setup of the thermal contact conductance as a function of interface clearance in the 2D FE model.

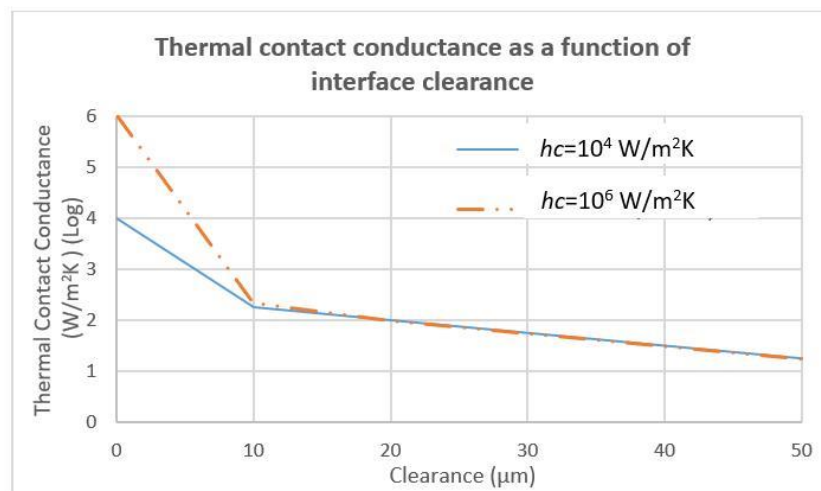


Figure 4. Set up of thermal contact conductance versus interface clearance.

3.3 Pad boundary condition

There are two boundary conditions in the literature that are commonly used for FE modelling of the pad's mechanical boundary condition.

- No-Rotation (NR) (maintain the pad with no rotational degree of freedom about the z-axis), as shown in Figure 2. This assumes that there is no friction induced bending moment effect.

- Free-Rotation (FR) that assumes the pad can rotate freely about the z -axis at the pivot point A, as indicated in Figure 2, which is 15 mm above the friction interface [20].

Arguably neither of these two conditions represent the true dynamic behaviour of brake pads in a real braking event. The pad is normally under a restricted Free-Rotation (FR) condition, i.e. it can rotate slightly about the z -axis due to the friction/reaction forces and clearance fit between the pad and the caliper in a braking event. Consequently, the disc-pad interface contact pressure and temperature distributions can be affected. A limited rotational effect is realised in this paper by selecting the pivot point D, which is 5 mm above the friction interface (as indicated in Figure 2). This setting provides the pad with limited rotational degree freedom (LR) that mimics a certain level of the friction induced bending moment effect on braking behaviour (see Table 1, 2D FE Model settings).

4 Results and discussion

4.1 Effect of pad rotation degree of freedom

4.1.1 No-Rotation (NR) and Free-Rotation (FR) boundary conditions

The effect of NR and FR boundary settings is assessed first, shown in Figure 5, where the x -axis represents the pad contact surface from its trailing edge (0) to its leading edge (1). The results shown in Figures 5 and 6 are obtained at $t = 33$ ms, which is equivalent to one revolution of the brake disc with respect to the stationary brake pad [27,36]. Figures 5(a) and 5(b) show results with normal and high thermal contact conductance, respectively.

Figure 5(a) indicates that, under a NR boundary condition, the pad pressure and surface temperature are distributed nearly uniformly at the interface (at about 100°C and 1 MPa). However, with the FR condition both the pressure and temperature change significantly (the

pressure changes from about 0 MPa at the trailing edge to about 6 MPa at the leading edge and the temperature increases from about 20°C at the trailing edge to about 500°C at the leading edge). Figure 5(b) shows that the pad pressure is nearly uniformly distributed at the interface under a NR boundary condition, but changes significantly under a FR boundary condition (from 0 to 7MPa). As far as temperature is concerned, both NR and FR conditions affect the distributions significantly at high thermal contact conductance. The pad temperature increases from 30°C at the trailing edge to a maximum 33°C at the middle of the contact region before decreasing to 25°C at the leading edge.

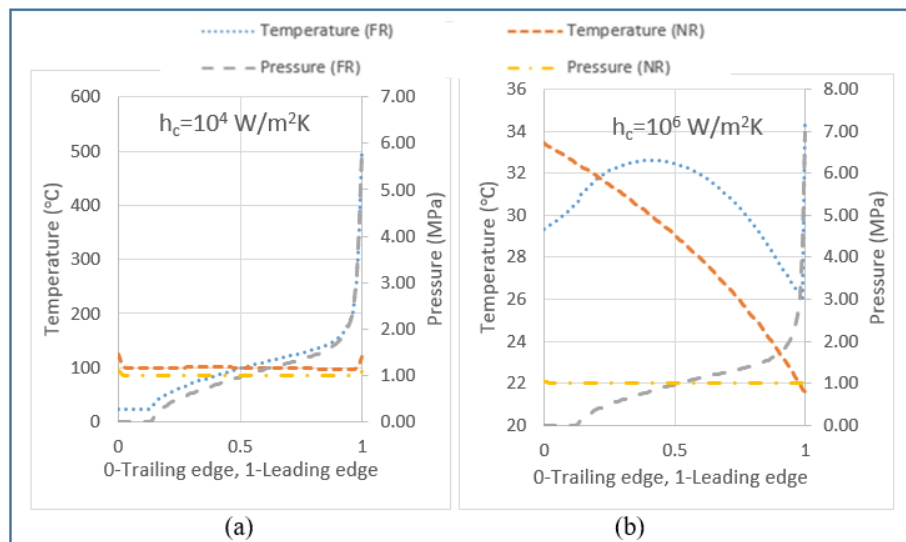


Figure 5. Pressure and temperature distributions with FR and NR at $t = 33 \text{ ms}$.

It is clear that the pressure distribution is significantly affected by the pad boundary condition (NR or FR) in both normal and high thermal contact conductance situations (Figure 5). Since NR does not represent actual brake pad conditions in braking and FR overestimates the effects of the friction induced bending moment on contact pressure, a limited rotational pad boundary condition should be considered in 2D-FE modelling/simulation of this type. The pivot point D, which is 5 mm from the friction interface (shown in Figure 2) is taken to

represent a limited rotational (LR) degree of freedom of the pad [36] and is used in setting the pad boundary condition in this work.

4.1.2 Limited-Rotation (LR) boundary condition

Figure 6 shows that the pressures at the pad/disc interface under an LR condition are higher at the leading side than the trailing side, due to the friction induced moment effect. Similarly, the temperature is higher at the leading side than the trailing side due to the combined effect of the contact pressure and the heat flux/transfer.

The results in Figures 5 and 6 shows that the magnitudes of the temperature and the pressure near the trailing edge and the leading edge normally change dramatically, e.g. Figure 5(a) shows that for the pressure under an FR condition, the pressure changes from 2 MPa to 7 MPa and the temperature changes from 200°C to 500°C within a region of 10% of the contact length adjacent to the leading edge. In order to extract more general trends from the 2D-FE simulation, in terms of how the thermal contact conductance affects the pad/disc interface heat partitioning and temperature distribution, the data near the leading and trailing edges are largely excluded in the remainder of this paper. Therefore, the results for 10% from the trailing edge and 10% from the leading edge are not included/presented in the results section. The x -axis shown in Figures 7-11 and 14 starts from 0.1 and ends at 0.9 of the pad contact surface.

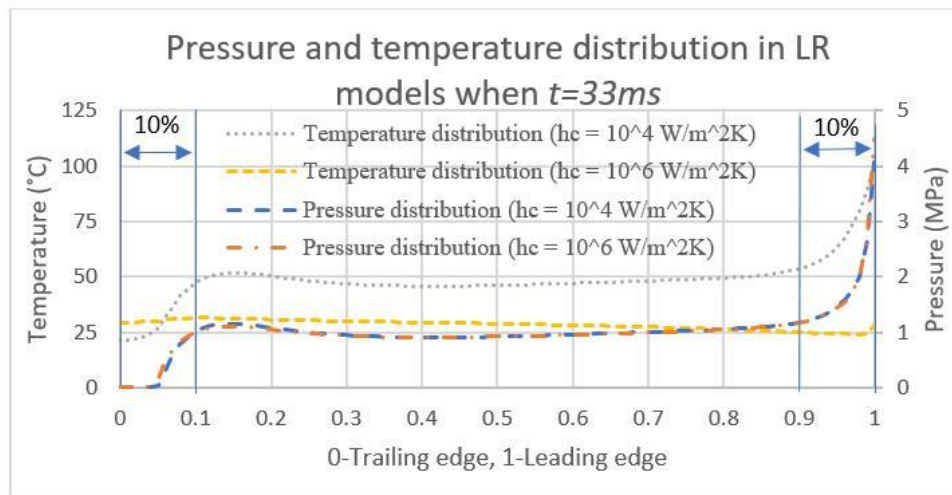


Figure 6. Pressure and temperature distributions in LR models with different thermal contact conductance values.

4.2 Effect of the thermal contact conductance

4.2.1 Interface temperatures

Due to the existence of an ITL at the brake pad/disc interface, the contact surface temperature of the pad will be different to that of the disc. Figure 7 shows simulation results under LR conditions.

As shown in Figure 7(a) the temperature at the disc side is about uniform at 110°C and the pad temperature slightly decreases from 253°C at the trailing side to 210°C in the middle before increasing to 240°C at the leading side, with a normal thermal contact conductance. The difference between pad temperature and disc temperature is about 130°C. By contrast, for high thermal contact conductance conditions the disc temperature decreases from the pad trailing side to the pad leading side, shown in Figure 7(b), and the difference between pad temperature and disc temperature is about uniform 2°C. From Figure 7(b), it is expected

that if $h_c \geq 10^6 \text{ W/m}^2\text{K}$, then the temperature difference at the interface becomes very small and can be ignored. By contrast, for $h_c \leq 10^4 \text{ W/m}^2\text{K}$ the temperature difference at the interface becomes very large, and the effect of h_c cannot be ignored.

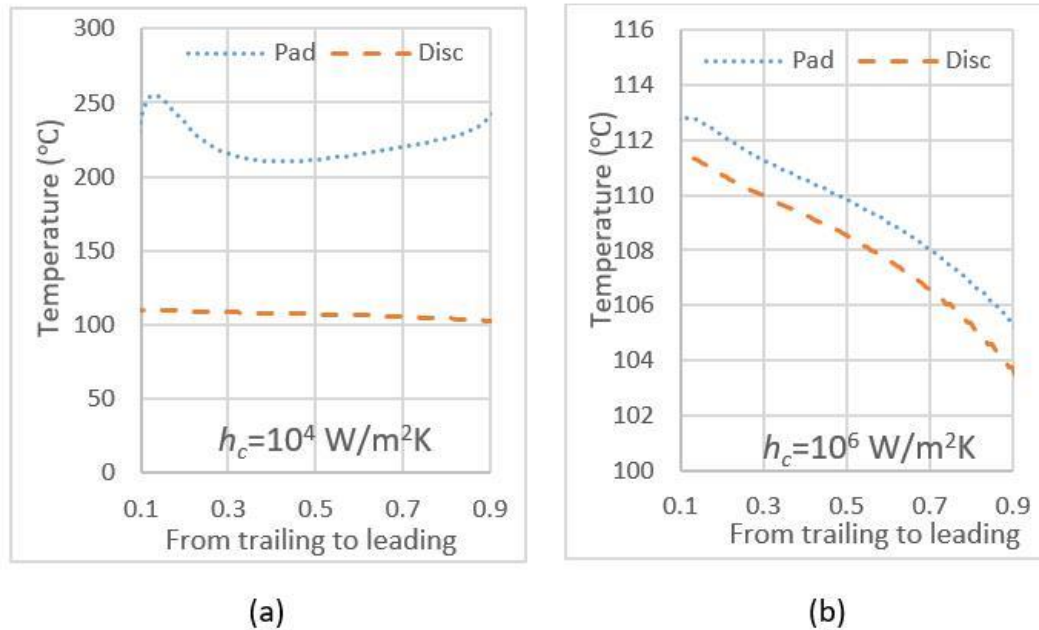
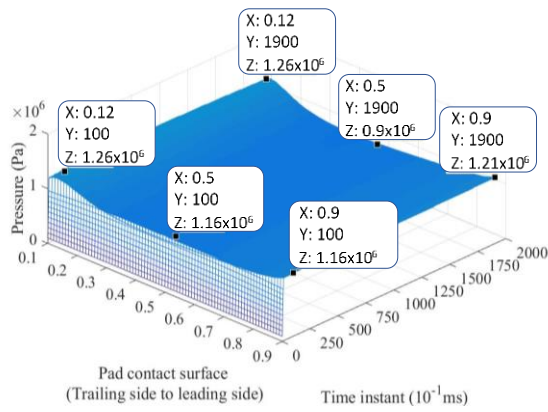


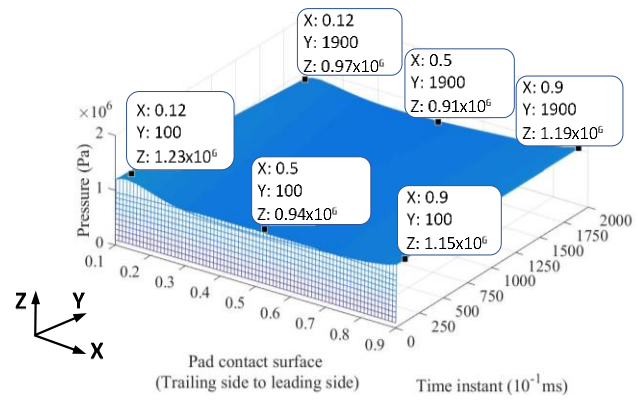
Figure 7. Temperature distribution in LR models with different thermal contact conductance values.

4.2.2 Pad contact pressure evolution

In order to understand the heat transfer behaviour during the friction sliding process, the application time is extended from 33ms (used in authors' previous work [27,36]) to 200ms. Figures 8 to 10 show the effect of the thermal contact conductance on contact pressures and temperatures over the sliding time period (from 0 to 200ms) under the LR boundary condition.



(a) Pad pressure distribution in LR model with normal thermal contact conductance



(b) Pad pressure distribution in LR model with high thermal contact conductance

Figure 8. Pressure distribution with different thermal contact conductance values (W/m^2k).

(a) $h_c = 10^4$; (b) $h_c = 10^6$.

Figure 8 shows the time variation of contact pressure as a function of sliding time. The pattern of pressure variation under normal and high thermal contact conductance are about the same, i.e. they do not change much with time and distribute fairly evenly along the contact length. For example, at the trailing side shown in Figure 8(a) the pressure with normal thermal contact conductance decreases slightly from 1.24 MPa at $t = 10$ ms to 1.22 MPa at $t = 190$ ms, and, comparably, the pressure with high thermal contact conductance decreases from 1.21 MPa at $t = 10$ ms to 0.864 MPa at $t = 190$ ms, shown in Figure 8(b).

4.2.3 Pad contact surface temperature evolution

Figure 9(a) shows that after the first 10ms, the temperature along the contact length decreases from the trailing side ($T = 143.3^\circ C$) to the middle ($T = 133^\circ C$), and then increases from the middle to the leading side ($T = 139.5^\circ C$). The temperature increases with sliding time. At $t = 190$ ms, the temperatures reach $249.2^\circ C$, $211.1^\circ C$ and $237.5^\circ C$, respectively, at the trailing side, the middle, and the leading side.

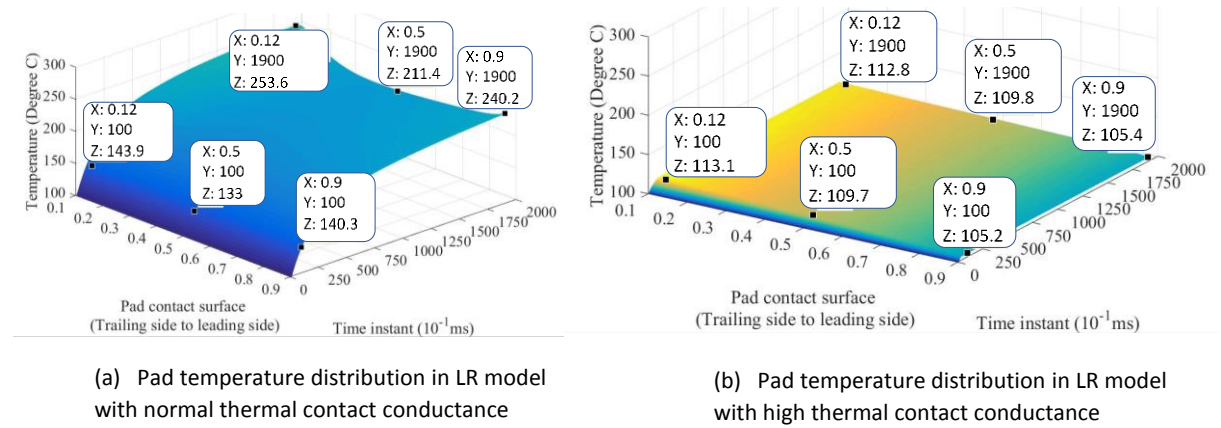


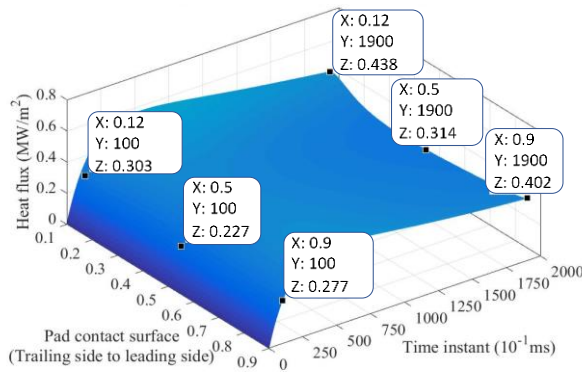
Figure 9. Temperature distribution with different thermal contact conductance values ($\text{W}/\text{m}^2\text{k}$). (a) $h_c = 10^4$; (b) $h_c = 10^6$.

Figure 9(b) shows that the temperature distribution with high thermal contact conductance has not changed as significantly as that under a normal thermal contact conductance condition (Figure 9(a)). For example, at the trailing side, the temperature is $T = 113.1^\circ\text{C}$ at $t = 10$ ms and $T = 112.8^\circ\text{C}$ at $t = 190$ ms. In addition, the temperature decreases linearly along the contact length, from 112.8°C at the trailing side to 105.5°C at the leading side when $t = 190$ ms.

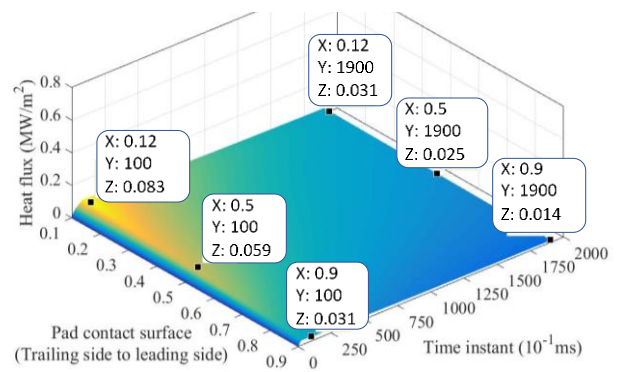
4.2.4 Pad contact surface heat flux evolution

Figure 10(a) shows that at $t = 10$ ms heat flux decreases from the trailing side ($0.299 \text{ MW}/\text{m}^2$) to the central region ($0.227 \text{ MW}/\text{m}^2$) then increases towards the leading side ($0.271 \text{ MW}/\text{m}^2$). At $t = 190$ ms, the heat flux decreases from the trailing side ($0.425 \text{ MW}/\text{m}^2$) to the central region ($0.314 \text{ MW}/\text{m}^2$) then increases towards the leading side ($0.394 \text{ MW}/\text{m}^2$). During the simulation, the maximum heat flux is $0.584 \text{ MW}/\text{m}^2$ and occurs at $t = 53$ ms on the trailing side.

Figure 10(b) shows the pad heat flux under high thermal contact conductance, which is much lower in comparison than under normal thermal contact conductance, Figure 10(a). The maximum heat flux is 82.9 kW/m^2 and occurs on the trailing side at $t = 10 \text{ ms}$, which is 7 times lower than what occurs with a normal thermal contact conductance. The heat flux decreases from the trailing side to the leading side along the contact surface axis as well as along the time axis, which is different from what occurs under a normal thermal contact conductance condition, shown in Figure 10(a).



(a) Pad heat flux distribution in LR model with normal thermal contact conductance



(b) Pad heat flux distribution in LR model with high thermal contact conductance

Figure 10. Heat flux into the pad with different thermal conductance values ($\text{W/m}^2\text{k}$). (a) $h_c = 10^4$; (b) $h_c = 10^6$.

4.3 Heat partition

In order to understand how heat transfers at the pad/disc interface during braking event, the heat fluxes to both the disc side and the pad side are presented in Figures 11-13.

4.3.1 Heat flux distribution along the contact interface

Figure 11(a) shows that the heat flux at the pad side changes slightly from the trailing to the leading side, as discussed previously with Figure 10(a) under normal thermal contact conductance conditions. The value decreases from 0.45 MW/m² at the trailing side to 0.275 MW/m² at the middle and then increases to about 0.4 MW/m² at the leading side. In contrast, Figure 11(b) shows that under a higher thermal contact conductance condition, the heat flux decreases linearly from 0.03 MW/m² at the trailing side to 0.01 MW/m² at the leading side as discussed previously with Figure 10(b).

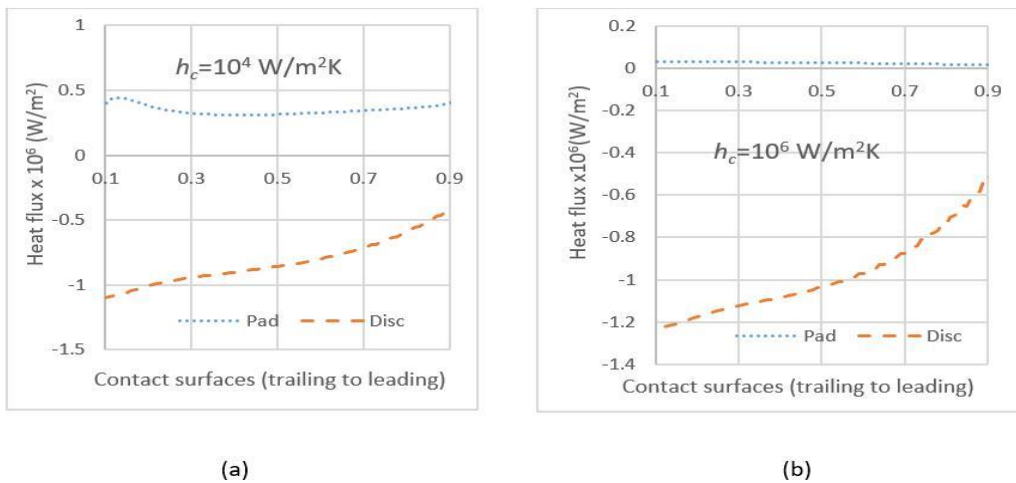


Figure 11. Heat flux distribution in LR models with different thermal contact conductance at $t = 33 \text{ ms}$

Figure 11 shows that the disc-side heat flux is not uniform, decreasing in magnitude from the pad trailing side to the leading side under both normal thermal contact conductance (1.1 MW/m² to 0.45 MW/m², shown in Figure 11(a)) and high thermal contact conductance (1.25 MW/m² to 0.5 MW/m², shown in Figure 11(b)). This indicates that heat dissipated into the disc increases as the disc slides through the pad/disc contact interface zone. The thermal contact conductance condition does not affect the magnitude of the heat flux to the disc as much as it does the magnitude of heat flux to the pad.

4.3.2 Heat flux at selected nodes on pad/disc contact surfaces

For further insight into the heat transfer behaviour at the disc/pad interface, three nodes on the pad bottom surface (labelled '135', '165' and '195' at the locations 'b', 'c' and 'd', respectively, as indicated in Figure 2) and the corresponding nine nodes at the top surface of the disc in three locations (labelled '3970, 4000, 4030', '4970, 5000, 5030' and '5970, 6000, 6030') are selected for analysis of the heat flux and partition ratio. Figures 12 and 13 show the temporal history of the heat flux as the disc block slides along the lower surface of the pad (illustrated in Figure 2).

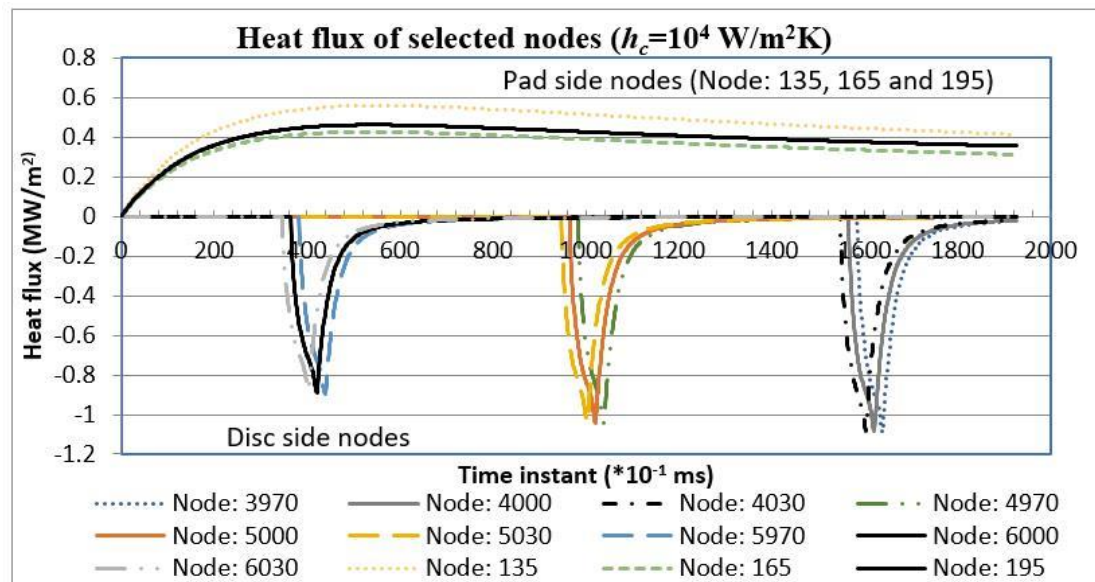


Figure 12. Heat flux at the selected nodes ($h_c = 10^4 \text{ W/m}^2\text{K}$).

Figure 12 shows that when the thermal contact conductance is $10^4 \text{ W/m}^2\text{K}$, the heat flux transfer to the pad side increases rapidly at the beginning, reaching a maximum of about 0.58 MW/m^2 after about 400 ms, and then decreases slowly. The heat flux to the disc side increases monotonically. In Figure 13, thermal contact conductance is $10^6 \text{ W/m}^2\text{K}$ and the heat flux to the pad side reaches its maximum value in a shorter time (about 100 ms). The

maximum heat flux to the pad side (less than 0.1MW/m^2) is much smaller than the value achieved for the normal thermal contact conductance model. The heat flux to the disc side reaches its maximum value in a shorter time, then decreases through the simulation.

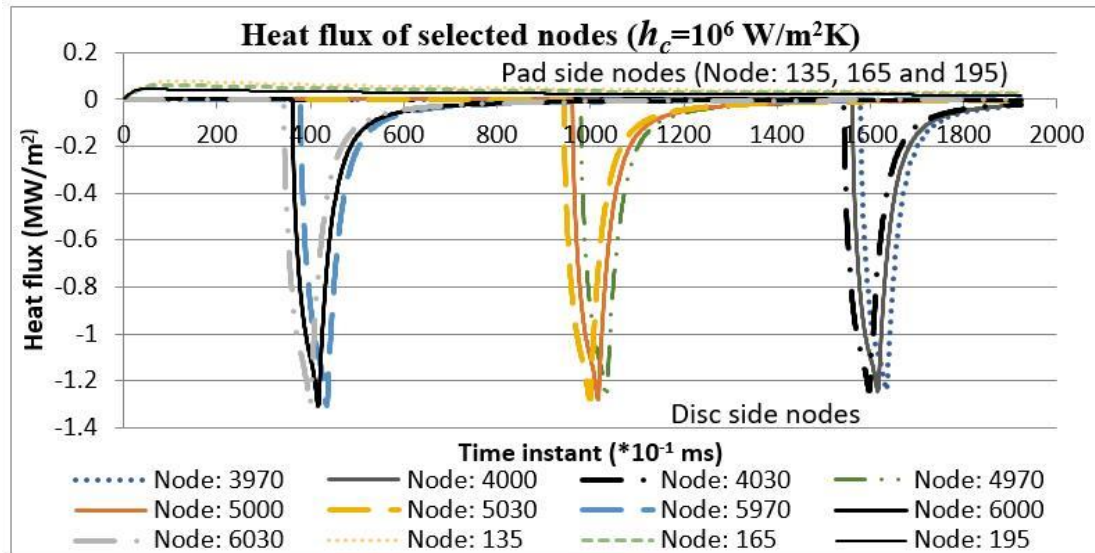
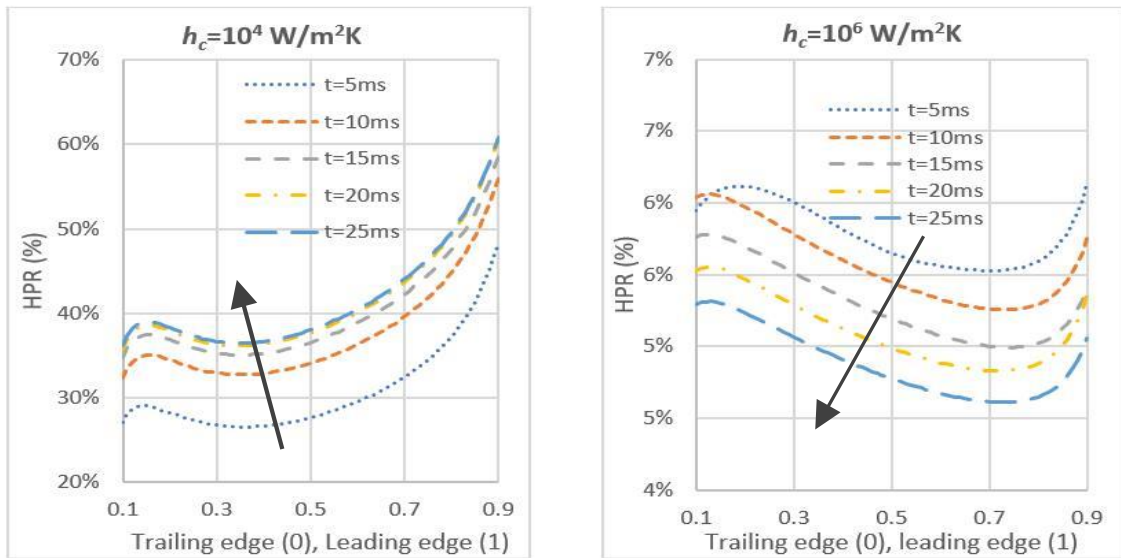


Figure 13. Heat flux of selected nodes ($h_c = 10^6 \text{ W/m}^2\text{K}$).

4.3.3 Heat partition ratio at different time instant

Five snap-shot times have been selected during the simulation (5 ms, 10 ms, 15 ms, 20 ms, and 25 ms) at which heat flux data is plotted and the heat partition ratio is calculated, shown in Figure 14. Figure 14(a) shows the heat partition ratio under a normal thermal contact conductance condition. It increases slightly at the trailing side then decreases and increases again along the contact surface. It also shows the heat partition ratio increases rapidly at the beginning, reaching a value of around 36% at 25 ms. In comparison, Figure 14(b) shows the heat partition ratio under a high thermal contact conductance model decreases from the trailing side to the leading side. The heat partition ratio decreases from about 6% to 5% within the first 25 ms of the braking event studied.



(a)

(b)

Figure 14. Evolution of heat partition ratio under an LR condition.

4.4 Discussion

In friction braking, a tribo-layer is formed at the pad/disc interface after a burnishing/bedding-in process that improves braking performance in general and moderates the friction heat transfer at the pad and disc interface, as shown by the 2D FE simulation. Specifically, the pad surface temperature distribution differs significantly under certain thermal contact conductance conditions, as shown in Figure 7, suggesting that for FE modelling/analysis the interface thermal condition must be carefully considered in order to obtain accurate simulation results as far as friction surface temperature and heat dissipation are concerned. Notably, the thermal contact conductance does not have much effect on the pressure distribution, shown in Figure 6.

4.4.1 Heat fluxes in the pad and disc

Figure 11 shows that the heat flux at the disc side is non-uniform and decreases in magnitude from the pad trailing side (1.1 to 1.25 MW/m²) to the pad leading side (0.45 to 0.5 MW/m²) under normal and high thermal contact conductance conditions. These observations indicate that the heat flux increases as the disc slides through the pad/disc contact interface zone (from the leading side to the trailing side) under both normal and high thermal contact conductance conditions.

Figure 11 shows clearly that the thermal contact conductance significantly affects the heat dissipated into the pad, e.g. the average heat flux to the pad under normal thermal contact conductance condition (around 0.35 MW/m²) is about 17 times higher than that under higher thermal contact conductance conditions (around 0.02 MW/m²) at $t = 33$ ms. Comparably, the thermal contact conductance condition does not have much effect on the magnitude of the heat flux into the disc (indicated in Figure 11).

4.4.2 Heat partition models

Based on the thermal properties of the contact pairs and the contact area ratio shown in Tables 1 and 2, the heat partition ratio is estimated at 1% and 13%, respectively, by using equations (5) and (6). In contrast, based on the simulation results shown in Figures 12-14, about 30% of the heat flux goes to the pad side and 70% goes to the disc side under normal thermal contact conductance. For high thermal contact conductance, however, the heat partition ratio is about 5% to the pad side and 95% to the disc side. It is clear that the traditional partition ratio equations (5) and (6) provide a rather poor prediction as far as a friction braking process is concerned.

As pointed out by Komanduri and Hou [30], equations (5) and (6) enforce an equal temperature condition at the friction interface. For an often-repeated braking sequence where the heat is transferred to remote bodies, the semi-infinite body assumption used to

develop the equations no longer adequately represents the disc brake friction. Figures 12 and 14 indicate that the thermal system takes a longer time to reach a thermally steady situation under normal contact conductance conditions. This is particularly significant, as far as friction braking systems are concerned, because it is known that a normal braking event is short (generally within 5-15 seconds). Under such a time scale, the magnitude of h_c can significantly affect the heat transfer state, i.e. whether it is largely in steady state or in a transient state during a normal braking event.

The existence of an ITL formed after burnishing and/or bedding-in with a comparably large interface contact area makes the interface thermal contact conductance a more significant issue in analysis of friction braking processes in comparison with analyses of other types of friction processes/systems, such as bearing/gearing and forming/machining processes.

It is debatable just what f value should be used in study of friction braking processes and there is limited information available in literature. In this work $f = 0.75$ is used, which is discussed in section 2.4. Further research on this issue is necessary.

5 Conclusions

Simulation results based on the 2D FE model developed in this work show how factors such as heat generation ratio f , thermal contact conductance h_c , friction pairs material properties (particular their thermal properties) and friction pairs boundary conditions (mechanical and thermal), affect the heat transfer in a friction braking process. It is found that

- i. the pad boundary conditions (NR, LR and FR) mainly affect the interface pressure distribution, which in turn affects the interface temperature distribution;

- ii. the interface thermal contact condition, as well as the pad boundary condition, affects the pad temperature and disc temperature at the contact interface. The pad/disc temperature difference at the interface can be as small as 2°C and as large as 130°C under the conditions studied in this work;
- iii. the transient heat partition in friction braking is clearly much different to the conventional friction-pair steady heat partition (which assumes two semi-infinite bodies in contact with zero thermal contact resistance). The heat partition ratio is not uniformly distributed along the interface under the thermal contact conditions studied in this work;
- iv. The heat partition ratio reaches a steady stage (~6%) within very short time period ($t \approx 20$ ms) under high thermal contact conductance condition (i.e. $h_c = 10^6$ W/m²K). It takes, however, a much longer time to reach the steady state under normal thermal contact conductance condition (i.e. $h_c = 10^4$ W/m²K). It is clear that thermal contact conductance, h_c , affects the heat flux distribution, interface temperature distribution at the pad/disc interface during braking process as well as the heat transfer state.

Even though values of h_c from 10^3 to 10^5 W/m²K are reported in literature, it is still debatable just what is a good estimate of the normal thermal contact conductance for friction braking applications. Further experimental investigations are necessary for better understanding and quantification of this important feature. Similarly, some further research on f value is necessary, and it is anticipated that the thermal contact conductance, h_c , and the heat generation ratio, f , have a combined effect on the state of heat transfer in friction braking processes.

Declaration of conflicting interests

The Authors declare that there are no conflicts of interest.

References

- [1] Hwang. P, Wu. X, Investigation of temperature and thermal stress in ventilated disc brake based on 3D thermos-mechanical coupling model, *Journal of Mechanical Science and Technology* 24 (2010) 81-84
- [2] Talati. F, Jalalifar. S, Analysis of heat conduction in a disk brake system, *Heat Mass Transfer* (2009) 45: 1047-1059
- [3] Gao. C.H., Lin. X.Z., Transient temperature field analysis of a brake in a non-axisymmetric three-dimensional model, *Journal of Materials Processing Technology* 129 (2002) 513-517
- [4] Yang. YC, Estimation of thermal contact resistance and temperature distributions in the pad/disc tribosystem, *International Communication in Heat and Mass Transfer* 38 (2011) 298-303
- [5] Lee. K, Numerical prediction of brake fluid temperature rise during braking and heat soaking, *SAE Technical Paper Series*, 1999-01-0483
- [6] A.J. Day, T.P. Newcomb, Dissipation of frictional energy from the interface of an annular disc brake, *Proc. Inst. Mech. Eng. D: Transp. Eng.* 198 (11) (1984) 201–209.
- [7] A. Day, Chapter 7 – Thermal Effects in Friction Brakes, *Braking of Road Vehicles*, Elsevier Inc. 2014, Pages 215–258.
- [8] M.M. Abd-Rabou, M.G. El-Sherbiny, Thermo elastic study on brake pads using FEA, *J. Eng. Appl. Sci.* 45 (5) (1998) 709–719.
- [9] P. Dufrenoy, D. Weichert, Prediction of railway disc brake temperatures taking the bearing surface variation into account, *Proc. Inst. Mech. Eng.F: Rail Rapid Transit* 209 (1995) 67–76.

- [10] Tirovic M., Day A. J., Newcomb T. P., Disc brake interface pressure distributions. Proc. Instn Mech. Engrs, Part D, 1991, 205(D2), 137–146A.
- [11] Floquet, M.C. Dubourg, Non-axisymmetric effects for three-dimensional analysis of a brake, Trans. ASME, J. Tribol. 116 (1994) 401–408.
- [12] Loizou, A., Qi, H.S. & Day, A.J. A numerical and experimental study of the factors that influence heat partitioning in disc brakes, FISITA2010-SC-P-26
- [13] M. Eriksson, S. Jacobson, Tribological surfaces of organic brake pads, Tribol. Int. 33 (2000) 817–827.
- [14] Qi, H.S., Day, A.J., Investigation of disc/pad interface temperatures in friction braking, Wear 262 (2007) 505–513
- [15] Noriyuki Hayashia, Akihiko Matsui, Sadamu Takahashi, Effect of surface topography on transferred film formation in plastic and metal sliding system, Volumes 225–229, Part 1, April 1999, Pages 329-338.
- [16] Okamura, T., Yumoto, H., Funddamental study on thermal behavior of brake discs, in 24th Annual Brake Colloquium & Exhibition. 2006, SAE International: Texas.
- [17] Piyush Chandra Verma, Rodica Ciudin, Andrea Bonfanti, Pranesh Aswath, Giovanni Straffelini, Stefano Gialanella, Role of the friction layer in the high-temperature pin-on-disc study of a brake material, Wear, 346–347 (2016), 56-65
- [18] G.A. Berry, J.R. Barber, The division of frictional heat — a guide to the nature of sliding contact, Journal of Tribology 106 (1984) 405–415.
- [19] Gopal. V, Thermal contact conductance and its dependence on load cycling, International Journal of Heat and Mass Transfer 66 (2013) 444-450
- [20] Loizou, A., Modelling and simulation of thermos-mechanical phenomena at the friction interface of a disc brake, PhD thesis, School of Engineering, Design & Technology, University of Bradford (2012)

- [21] Majcherczak, D., P. Dufrenoy, and M. Nait-Abdelaziz, Third body influence on thermal friction contact problems: Application to braking. *Journal of Tribology-Transactions of the ASME*, 2005. 127(1): p.89-95
- [22] Chantrenne. P, Raynaud. M, A microscopic thermal model for dry sliding contact, *Internal Journal of Heat Mass Transfer*, Vol. 40, No. 5, pp. 1083-1094, 1997
- [23] Yevtushenko A., Kuciej M., Och E., Yevtushenko O., Effect of the thermal sensitivity in modelling of the frictional heating during braking, *Advances in Mechanical Engineering* 8(12) · December 2016
- [24] Madhusudana, Y.L.C., Leonardi. E, On the enhancement of the thermal contact conductance: effect of loading history, *J. Heat transfer* 122 (2000) 46-49
- [25] M. Rosochowska, R. Balendra, K. Chodnikiewicz, Measurements of thermal contact conductance, *Journal of Materials Processing Technology* 135 (2003) 204–210
- [26] Shailendra K. Parihar and Neil T. Wright, Thermal Contact Resistance at Elastomer to Metal Interfaces, *Int. Comm. Heat Mass Transfer*, Vol. 24, No. 8, pp. 1083--1092, 1997
- [27] Qiu, L., Qi, H.S., Wood, A.S., A new paradigm for disc-pad interface models in friction brake system, EB2015-TEF-012, EuroBrake 2015
- [28] Blok H. Theoretical study of temperature rise at surfaces of actual contact under oiliness lubricating condition, in: *Proceedings of the General Discussion on Lubrication and Lubricants*, Institute of Mechanical Engineers, London, Vol. 2, 1937, pp. 222-235.
- [29] Carslaw, H.S. and Jaeger, J.C., *Conduction of Heat in Solids*, 2nd edition, Oxford Press, 1959
- [30] Komanduri. R, Hou. Z.B., Analysis of heat partition and temperature distribution in sliding systems, *Wear* 251 (2001) 925-938
- [31] S.A. Schaaf, On the superposition of a heat source and contact resistance, *Quarterly of Applied Mathematics* 5 (1) (1947) 107–111.

- [32] Nosko O., Partition of friction heat between sliding semi-spaces due to adhesion-deformational heat generation, *International Journal of Heat and Mass Transfer* 64 (2013) 1189–1195
- [33] J.R. Barber, The conduction of heat from sliding solids, *International Journal of Heat and Mass Transfer* 13 (1970) 857–869.
- [34] Ostermeyer, G.P., On the dynamics of the friction coefficient, *Wear* 254 (2003) 852-858
- [35] Loizou, A., Qi, H.S., Day, A.J. A., A fundamental study on the heat partition ratio of vehicle disc brakes, *ASME, J. Heat Transfer* 135, 121302 (2013), doi:10.1115/1.4024840
- [36] Qiu, L., Qi, H.S., Wood, A.S., Analysis of the interface heat partition in a friction brake system with 2D FE models, EB2016-FBR-016, EuroBrake 2016